Int. J. Multiphase Flow Vol. 13, No. 1, pp. 1–12, 1987
Printed in Great Britain.

0301-9322/87 $3.00 + 0.00

A UNIFIED MODEL FOR PREDICTING FLOW-PATTERN TRANSITIONS FOR THE WHOLE RANGE OF PIPE INCLINATIONS

D. BARNEA

Faculty of Engineering, Department of Fluid Mechanics and Heat Transfer, Tel-Aviv University, Ramat-Aviv 69978, Israel

(*Received* 2 *February* 1986; *in revised form* 9 *June* 1986)

Abstract—Models for predicting flow-pattern transitions in steady gas–liquid flow in pipes are summarized and presented. These models incorporate the effect of fluid properties, pipe size and the angle of inclination in a unified way that is not restricted to a specific range of pipe inclinations. Transition mechanisms are presented for each individual boundary and a logical path for systematic determination of the flow patterns is suggested.

INTRODUCTION

In the last few years many efforts have been directed towards the development of physical models that allow the analytical prediction of the flow patterns and the transition boundaries in steady-state two-phase gas–liquid flow. These models try to represent the true physics which is observed in experiments. They do, however, simplify the description of the physical phenomena so that a mathematical simulation is possible. The main purpose is to construct a completely general method that allows the prediction of the flow pattern, once the flow rates, the conduit geometry, the inclination angle and the fluid properties are specified. This aim has not been fully achieved as yet. A complete physical understanding of the phenomena related to flow-pattern transitions is still lacking. Nevertheless, substantial progress has been made in this field. Most of the models presented so far are restricted to a specific range of pipe inclinations and thus give only a partial view of the transition mechanisms in tubes.

Models for the following particular situations have been presented:

—horizontal and slightly inclined tubes (Taitel & Dukler 1976a; Husain & Weisman 1978; Kadambi 1982; Lin & Hanratty 1986);
—vertical upward flow (Taitel *et al.* 1980; Mishima & Ishii 1984; McQuillan & Whalley 1985);
—vertical downward flow (Barnea *et al.* 1982a);
—inclined upward flow (Barnea *et al.* 1985);
—inclined downward flow (Barnea *et al.* 1982b).

These models include a variety of mechanisms that explain the physical basis for the transitions. The transition mechanisms presented for horizontal flow differ considerably from those suggested for vertical flow. These mechanisms were modified and extended to include the effect of small deviations from the horizontal or vertical cases. The main difficulty arises in determining the range in which these extensions take place. At a given angle of inclination competing mechanisms may arise and it is not always clear which of these mechanisms is operative.

A comprehensive model for predicting flow-pattern transitions should incorporate the angle of inclination in such a way that a smooth change in mechanisms is obtained as the pipe inclination varies over all possible angles of inclinations.

Recently Barnea (1986) presented unified models for the transition from annular to intermittent flow and from dispersed bubble flow. The effect of inclination is integratively incorporated in these models.

Based on this work and on previously published models it appears that a satisfactory and consistent theory is available that can predict the steady-state transition boundaries for the whole

range of pipe inclinations. Thus it seems that a comprehensive systematic summary of the aforementioned models is now appropriate and is the basis for this work. In this summary a smooth change in mechanisms is presented as the angle of inclination is changed over all possible upward and downward angles of inclination and the problem of "switching" between two different mechanisms or selecting the applicable one is eliminated.

This presentation is not intended to be a review of all previous work but rather presents a preferred view of the relevant models that are best suited for the prediction of the flow pattern in a concise manner.

In what follows, transition mechanisms for each individual boundary will be presented. The transition criteria will be given for each transition in the form of either algebraic equations or dimensionless maps, where the equations are too complex for direct calculation. These equations or maps incorporate the effect of flow rates, fluid properties, pipe size and the angle of inclination. Thereafter a logical path for a systematic determination of the flow pattern will be presented.

THE TRANSITION FROM DISPERSED BUBBLES

Dispersed bubble flow usually appears at very high liquid flow rates. There are, however, conditions where small discrete bubbles also appear at low liquid rates. These bubbles are sometimes designated as bubble or bubbly flow. The distinction between bubbly and dispersed bubble flow is not always clearly visible. Dispersed bubble flow is observed over the whole range of pipe inclinations, while the bubbly flow pattern is observed only in vertical and off-vertical flows in relatively large diameter tubes. The bubbly flow pattern can exist provided two conditions are met:

(1) The Taylor bubble velocity exceeds the bubble velocity. This condition is satisfied in large-diameter pipes (Taitel *et al.* 1980):

$$D > 19\left[\frac{(\rho_L - \rho_G)\sigma}{\rho_L^2 g}\right]^{\frac{1}{2}}, \qquad [1]$$

where D is the tube diameter, ρ_L and ρ_G are the liquid and gas densities and σ is the surface tension.

(2) The angle of inclination β (from the horizontal) is large enough to prevent migration of bubbles to the top wall of the pipe (Barnea *et al.* 1985):

$$\frac{\cos\beta}{\sin^2\beta} = \tfrac{3}{4}\cos 45^\circ \frac{U_0^2}{g}\left(\frac{C_L\gamma^2}{d}\right), \qquad [2]$$

where U_0 is the bubble rise velocity, C_L is the "lift" coefficient and γ is the distortion coefficient of the bubble. U_0 is given by the relation (Harmathy 1960)

$$U_0 = 1.53\left[\frac{g(\rho_L - \rho_G)\sigma}{\rho_L^2}\right]^{\frac{1}{4}}. \qquad [3]$$

The average value suggested for C_L is 0.8 (Streeter 1961) and γ ranges from 1.1 to 1.5 (based on observation).

When these two conditions are satisfied, bubbly flow is observed even at low liquid rates were turbulent forces do not cause bubble breakup. Taitel *et al.* (1980) showed that the transition from bubbly to slug flow takes place when the gas void fraction exceeds a critical value of $\alpha_c = 0.25$. This transition is given by

$$U_{LS} = \frac{1-\alpha}{\alpha}U_{GS} - 1.53(1-\alpha)\left[g\frac{(\rho_L - \rho_G)\sigma}{\rho_L^2}\right]^{\frac{1}{4}}\sin\beta, \qquad [4]$$

where $\alpha = \alpha_c = 0.25$. The angle β is positive for upward flow and negative for downward flow.

At high liquid flow rates dispersed bubbles exist even for $\alpha > 0.25$, due to turbulence which causes bubble breakup and prevents agglomeration. The transition mechanism from the dispersed bubbles was first suggested by Taitel *et al.* (1980) for upward vertical flow and recently modified

by Barnea (1986) to account for pipe inclination. The result is

$$d_C \geq \left[0.725 + 4.15\left(\frac{U_{GS}}{U_M}\right)^{\frac{1}{2}}\right]\left(\frac{\sigma}{\rho_L}\right)^{\frac{3}{5}}\left(\frac{2f_M}{D}U_M^3\right)^{-\frac{2}{5}}, \quad [5]$$

where U_M is the mixture velocity and f_M is the friction factor based on the mixture velocity. The bubble diameter on the transition boundary, d_C, is a function of the liquid velocity and the angle of inclination. The value of d_C is taken as the smallest between d_{CD} and d_{CB}, where d_{CD} is the critical bubble size above which the bubble is deformed,

$$d_{CD} = 2\left[\frac{0.4\sigma}{(\rho_L - \rho_G)g}\right]^{\frac{1}{2}}; \quad [6]$$

and d_{CB} is the critical bubble size below which migration of bubbles to the upper part of the pipe is prevented,

$$d_{CB} = \frac{3}{8}\left[\frac{\rho_L}{\rho_L - \rho_G}\right]\frac{f_M U_M^2}{g\cos\beta}. \quad [7]$$

The transition boundary [5] is valid for $0 \leq \alpha \leq 0.52$. At the upper limit the maximum volumetric packing density of the bubbles is reached and coalescence occurs even at high turbulent levels. The transition curve that characterizes this condition is

$$U_{LS} = U_{GS}\frac{1-\alpha}{\alpha}, \quad [8]$$

where $\alpha = 0.52$.

Once the fluid properties and pipe geometry are specified, the theoretical transition curves can be plotted on U_{LS} vs U_{GS} coordinates. Such curves are shown in figures 1 and 2 for the air–water system at 25°C and 0.1 MPa. Curve B represents the transition from bubbly flow [4], while transitions D and G ([5] and [8], respectively) designate the transition from dispersed bubble flow. It should be noted that transition B is not observed at all in small-diameter pipes, as predicted by [1], and at angles of inclination below that predicted by [2]. At relatively large diameter pipes and steep inclinations (figure 1, $\beta = 80, 90, -80, -90$), the bubble flow pattern is seen to exist in two zones. In the zone to the left of curve B and below D the presence of deformable bubbles which move upward with a zig-zag motion is predicted. In the second zone above curve D and to the left of curve G a more finely dispersed bubble system is observed.

THE STRATIFIED–NONSTRATIFIED TRANSITION

For horizontal and slightly inclined tubes, Taitel & Dukler (1976a) suggested that transition from equilibrium stratified flow is due to Kelvin–Helmholtz instability. They considered stratified flow with a finite wave on the surface over which the gas flows. As the gas accelerates over the wave crest, the pressure in the gas phase decreases due to the Bernoulli effect and the wave tends to grow. On the other hand, the force of gravity acting on the wave tends to cause it to decay. Taitel & Dukler (1976a) suggested that the criterion at which the wave will grow and at which the transition from stratified flow occurs is

$$F^2\left[\frac{1}{(1-\tilde{h}_L)^2}\frac{\tilde{U}_G^2\frac{d\tilde{A}_L}{d\tilde{h}_L}}{\tilde{A}_G}\right] \geq 1 \quad [9]$$

where F is a Froude number modified by the density ratio:

$$F = \sqrt{\frac{\rho_G}{\rho_L - \rho_G}}\frac{U_{GS}}{\sqrt{Dg\cos\beta}}. \quad [10]$$

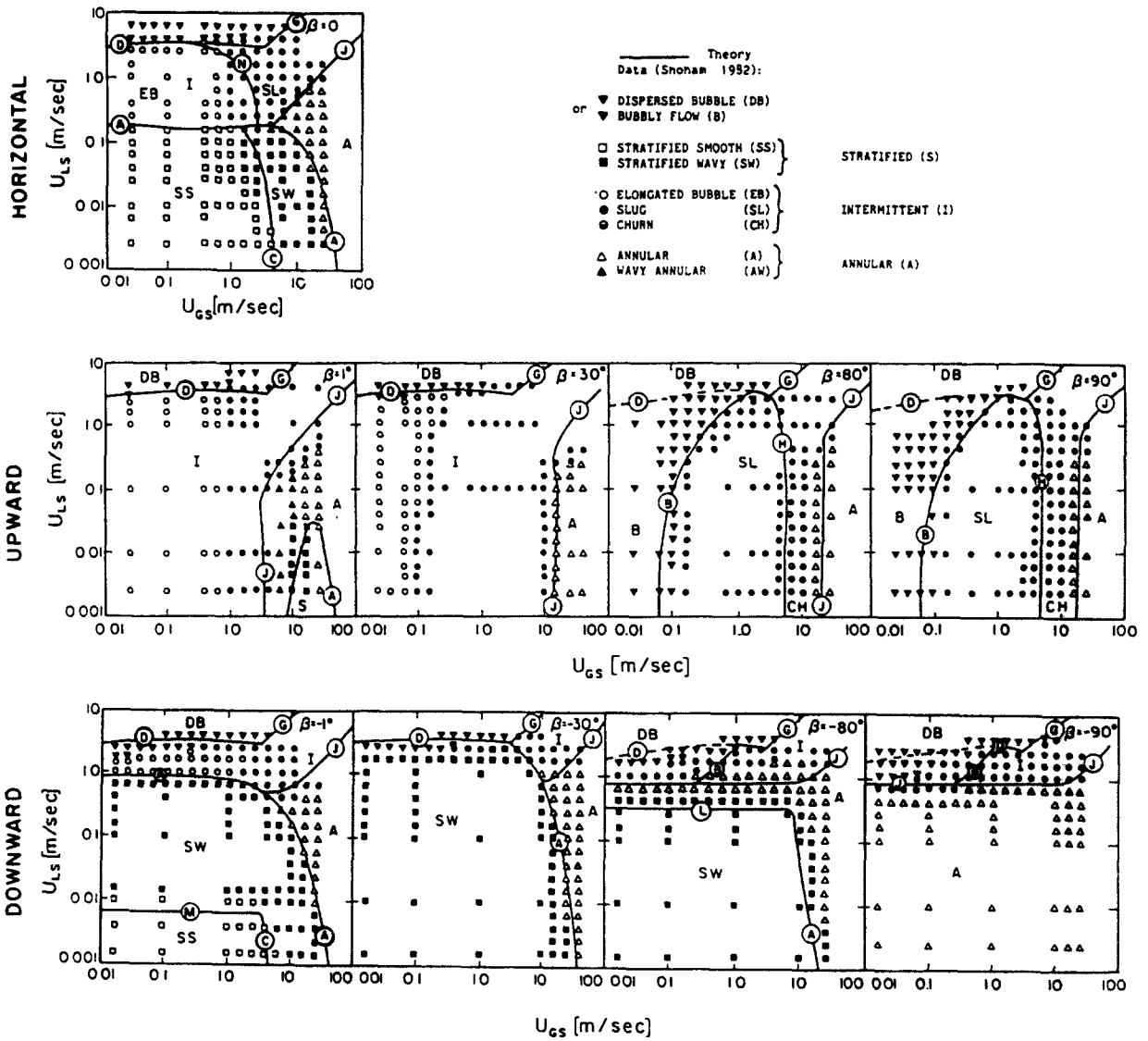

Figure 1. Flow-pattern maps for the whole range of pipe inclinations. Air–water, 0.1 MPa, 25°C, 5.1 cm dia.

The dimensionless variables are defined by

$$\tilde{h}_L = \frac{h_L}{D},$$

$$\tilde{A}_L = \frac{A_L}{D^2},$$

$$\tilde{A}_G = \frac{A_G}{D^2}$$

$$\tilde{U}_L = \frac{U_L}{U_{LS}} = \frac{A}{A_L}$$

and

$$\tilde{U}_G = \frac{U_G}{U_{GS}} = \frac{A}{A_G}, \qquad [11]$$

where h_L is the liquid level in equilibrium stratified flow, U_L and U_G are the liquid and gas velocities, A_L and A_L are the liquid and gas cross-sectional areas and D is the tube diameter.

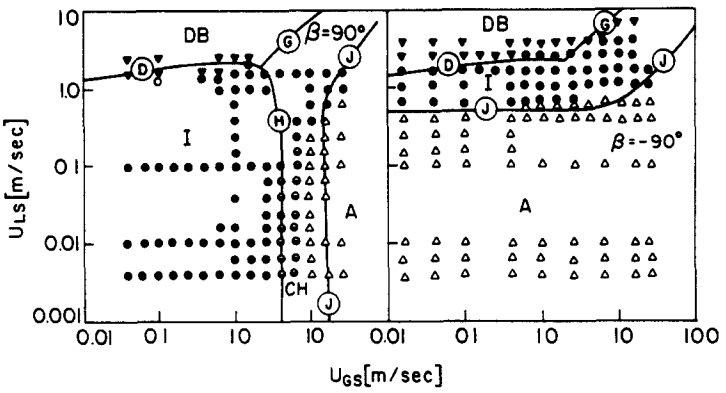

Figure 2. Flow-pattern maps for vertical upward and downward tubes. Air–water, 0.1 MPa, 25°C, 2.54 cm dia. Key as in figure 1.

Note that all the terms in the square brackets in [9] are functions only of $\tilde{h}_L$. Once the gas and liquid flow rates, fluid properties, inclination angle and pipe size are specified, the equilibrium liquid level can be found by solving the momentum equations for each phase in stratified flow (Taitel & Dukler 1976a). The equilibrium level is given in terms of X and Y:

$$X^2 = \frac{\frac{4}{D} f_{LS} \frac{\rho_L U_{LS}^2}{2}}{\frac{4}{D} f_{GS} \frac{\rho_G U_{GS}^2}{2}} = \frac{\left(\frac{dp}{dx}\right)_{LS}}{\left(\frac{dp}{dx}\right)_{GS}} \qquad [12a]$$

and

$$Y = \frac{(\rho_L - \rho_G) g \sin\beta}{\left(\frac{dp}{dx}\right)_{GS}}; \qquad [12b]$$

$(dp/dx)_S$ designates the pressure drop of one phase flowing alone in the pipe and f_S is the friction factor coefficient for a single-phase flow, which can be calculated by using the Moody diagram or equivalent correlations. Note that the friction factor f_S depends on the flow conditions (turbulent or laminar) as well as on the pipe roughness.

The equilibrium level $\tilde{h}_L$ as a function of X is shown in figure 3 for parameter values of Y. The results in figure 3 are for the case of turbulent liquid and gas flow in smooth pipes. It was shown, however (Taitel & Dukler 1976b; Taitel 1977), that to a good approximation, figure 3 can be used also for laminar–laminar and turbulent–laminar flows and for rough pipes. The effect of the flow conditions and roughness is taken into account in the parameters X and Y.

The transition criteria given by [9] is represented by curve A on a two-dimensionless map with F and $\tilde{h}_L$ as coordinates (figure 4). Once the physical properties, tube diameter and inclination angle are specified, the predicted transition line can also be plotted on U_{LS} vs U_{GS} maps.

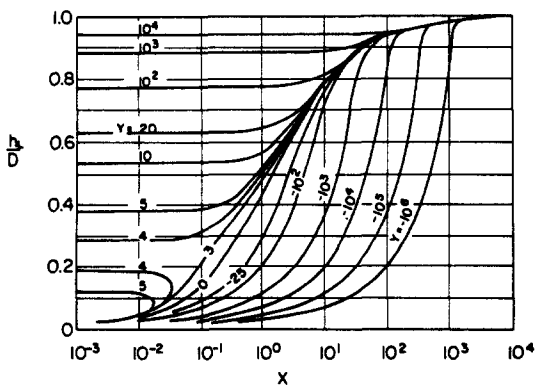

Figure 3. Equilibrium liquid level in stratified flow.

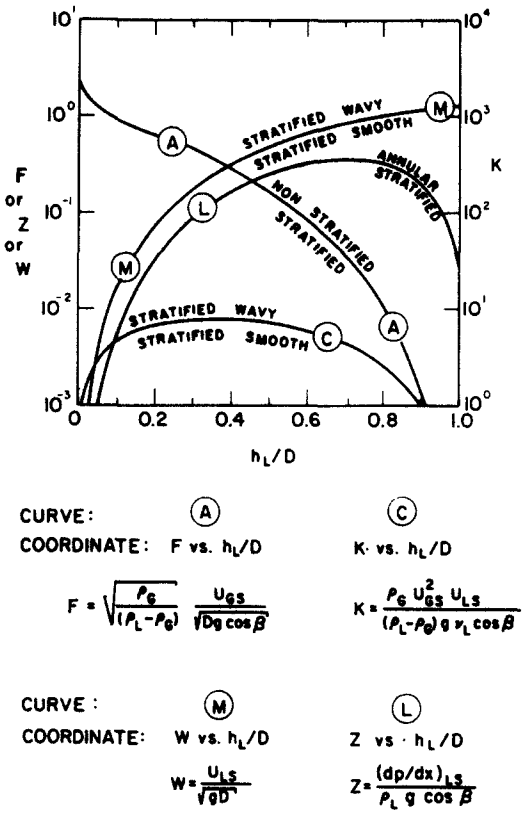

Figure 4. Generalized transition boundaries.

The results for an air–water system were compared with the experimental data of Shoham (1982) for the whole range of pipe inclinations and the agreement with the experimental results is satisfactory. Note, that small changes in the angle of inclination have a major effect on the stratified–nonstratified transition boundary A (figure 1). For slight upwards inclinations the stratified flow shrinks substantially (figure 1, $\beta = 1°$) and practically vanishes at intermediate angles of inclination (figure 1, $\beta = 30°$). This observation is also predicted very well by the theoretical transition A, which can also be used to predict the upward angle of inclination at which stratified flow disappears (in a specific region of flow rates). Changes in the downward inclination also have a profound effect on the stratified flow regime which expands considerably as the angle of inclination increases (figure 1, $\beta = 0°$, $-1°$, $-30°$). This phenomena is also predicted by the theoretical transition A.

Thus transition A is applicable in the whole range of pipe inclinations. However, the boundary curve A, may be terminated by either the transition to dispersed bubble (figure 1, $\beta = -30$) or by the stratified–annular boundary at downward inclinations and low gas flow rates (figure 1, $\beta = -80°$). In other words, in the region above the F vs $\tilde{h}_L$ curve (figure 4) stratified flow does not exist over the whole range of pipe inclinations, but in the region below it, subregions of dispersed bubble and annular flow may exist.

THE STRATIFIED–ANNULAR TRANSITION

Transition mechanism A ([9]) presents a criterion under which finite waves on stratified liquid flow are expected to grow resulting in either slug or annular flow. The region below curve A is expected to be stable stratified flow. However, at steep downward inclinations another mechanism comes into play, by which stable stratified flow is seen to change into annular flow at relatively low gas flow rates (Barnea *et al.* 1982b). This transition boundary is, thus, applicable only within the region bounded by curve A.

At high downward inclination angles the stratified liquid level is small and the liquid velocity (U_L) is very high. Under these conditions droplets are torn from the wavy turbulent interface and

may be deposited on the upper wall, resulting in an annular film. The condition for this type of annular flow to take place is (Barnea *et al.* 1982b)

$$U_L^2 \geqslant \frac{gD\,(1-\tilde{h}_L)\cos\beta}{f_L}, \qquad [13]$$

or in the dimensionless form

$$Z = \frac{\left(\frac{dp}{dx}\right)_{LS}}{\rho_L g \cos\beta} \geqslant 2\left(\frac{\tilde{A}_L}{\tilde{A}}\right)^2 (1-\tilde{h}_L)\frac{f_{LS}}{f_L}, \qquad [14]$$

where f_L is the liquid friction factor coefficient and f_{LS} the coefficient that refers to the case where the liquid flows alone in the pipe. For rough pipes and large Reynolds number $f_L/f_{LS} = 1$, while for smooth pipes $f_{LS}/f_L = (\tilde{D}_L \tilde{U}_L)^{-n}$, where $\tilde{D}_L$ is the liquid hydraulic diameter and n is a constant [equal to 0.2 for turbulent liquid flow and 1 for laminar flow (Taitel 1977)].

All quantities on the r.h.s. of [14] depend only on $\tilde{h}_L$. The curve describing the relation between Z and $\tilde{h}_L$ which satisfies [14] is designated as boundary L in figure 4. In the region below curve L stratified flow exists. Transition L is also plotted on a $U_{LS} - U_{GS}$ (figure 1, $\beta = -80$) map and shows good agreement with the experimental results. Transition L is shown to appear only at steep downward inclinations as stratified flow is changed gradually to annular flow. For the limiting case of vertical downward flow, $Z \to \infty$ ([14]), stratified flow disappears completely. For small angles of downward inclination and for upward inclinations transition L is outside the region bounded by transition A and therefore is not applicable. Thus, transition L can be checked and applied in the whole range of pipe inclinations.

THE TRANSITION FROM ANNULAR TO INTERMITTENT FLOW

A unified model that incorporates the effect of the angle of inclination was recently proposed by Barnea (1986) for the transition from annular to intermittent flow. This transition was assumed to occur when the gas core is blocked at any location by the liquid. Blockage of the gas core may result from two possible mechanisms:

(a) instability of the liquid film, due to partial downflow of liquid near the wall, causing blockage at the entrance;
(b) blockage of the gas core as a result of large supply of liquid in the film.

The condition for the instability of the liquid film in annular flow [mechanism (a)] was obtained from the simultaneous solution of the following dimensionless equations:

$$Y = \frac{1+75\,\alpha_L}{(1-\alpha_L)^{\frac{5}{2}}\alpha_L} - \frac{1}{\alpha_L^3}X^2 \qquad [15]$$

and

$$Y \geqslant \frac{2-\frac{3}{2}\alpha_L}{\alpha_L^3(1-\frac{3}{2}\alpha_L)}X^2; \qquad [16]$$

X and Y are defined as in [12a,b]. Equation [15] gives the steady-state solution for the liquid holdup, α_L, in annular flow. The value of α_L that satisfies the condition for the film instability is obtained from [16].

Blockage of the gas core by liquid lumps [mechanism (b)] will occur when the liquid supply in the film is large enough to provide the liquid needed to bridge the pipe. The condition for slugging was shown to be (Barnea 1986)

$$\frac{A_L}{A \cdot R_{sm}} = \frac{\alpha_L}{R_{sm}} \geqslant 0.5, \qquad [17]$$

where R_{sm} is the minimal liquid holdup within the formed liquid slug that will allow competent bridging of the gas passage. This minimum value is related to the maximum bubble volumetric

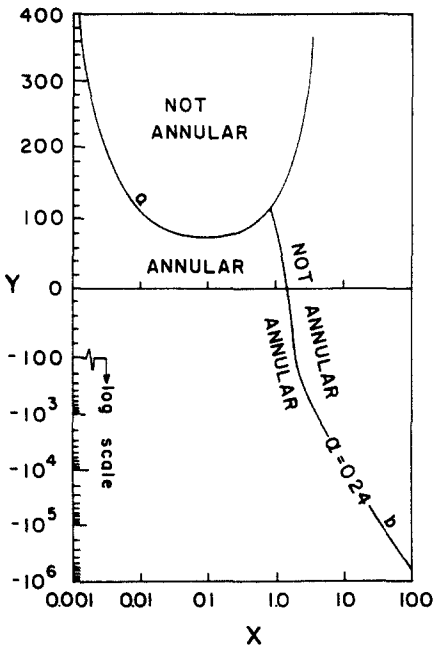

Figure 5. Generalized map for annular intermittent transition.

packing in the liquid slug and equals approx. 0.48. Lower values of R_s will make slugging impossible due to the high gas void fraction. Note, however, that this minimum value of $R_{sm} = 0.48$ is the actual slug holdup, R_s, on the annular–intermittent transition boundary in a very wide range of flow conditions. The calculation of R_s is discussed later in relation to [18].

The transition boundaries are shown in figure 5 in terms of the dimensionless coordinates X and Y. Solution of [15] and [16] yields the locus of X, Y pairs (line "a") along the stability curve [transition mechanism (a)]. The region below this curve is in stable annular flow, while the region above it yields unstable conditions, or intermittent flow. Equation [15] with the value of $\alpha_L = 0.5\, R_{sm}$ yields the condition where blockage occurs [mechanism (b)]. Equation [15] is plotted for a constant value of $\alpha_L = 0.24$ within the stable zone (the "b" lines). The region below curve "a" and to the left of curve "b" corresponds to annular flow.

The two mechanisms (a) and (b) mentioned above are both based on the characteristic film structure of annular flow. A smooth change in mechanisms is obtained either when the flow rates change, or when the pipe inclination varies over all possible angles.

The above transition criteria between annular and intermittent flow are mapped in figures 1 and 2 as transition boundary J and show good agreement with the experimental data. Note that the J line may be terminated by the stratified–nonstratified line (figure 4, $\beta = 0°$, $-1°$, $-30°$). Thus, the above proposed model is applicable only outside the range of stable stratified flow.

SUBREGIONS WITHIN THE INTERMITTENT FLOW

The intermittent pattern is usually subdivided into elongated bubble, slug and churn flows. Basically, these three flow patterns have the same configuration with respect to the distribution of the gas and the liquid interfaces. In these flow patterns slugs of liquid are separated by large bullet-shaped bubbles. In slug flow the liquid bridges are aerated by small gas bubbles. The elongated bubble pattern is considered the limiting case of slug flow when the liquid slug is free of entrained bubbles (Barnea & Brauner 1985), while the churn flow takes place when the gas void fraction within the liquid slug reaches a maximum value above which occasional collapse of the liquid slug occurs.

Recently Barnea & Brauner (1985) proposed a physical model for the prediction of gas holdup within the liquid slug (α_s or $1 - R_s$). It was suggested that the gas holdup on the transition line from dispersed bubbles is the maximum holdup that the liquid slug can accommodate as fully

dispersed bubbles at a given mixture velocity U_M ($= U_{GS} + U_{LS}$). Thus, curves of constant U_M within the intermittent region represent the locus where α_s is constant and is equal to the holdup of the dispersed bubble pattern at the transition boundary. Once the fluid properties and pipe size are set, α_s can be obtained from [5] to yield

$$\alpha_s = 1 - R_s = 0.058\left[d_C\left(\frac{2f_M}{D}U_M^3\right)^{\frac{2}{5}}\left(\frac{\rho_L}{\sigma}\right)^{\frac{1}{5}} - 0.725\right]^2; \quad [18]$$

when $\alpha_s = 0$ the elongated bubble–slug transition is obtained (Barnea & Brauner 1985). When the gas holdup within the liquid slug reaches the maximum bubble volumetric packing ($\alpha_s = 0.52$), the continuity of the very aerated liquid slug is destroyed by bubble agglomeration and the formation of regions of high gas concentration within the liquid slug, resulting in transition to churn flow (Brauner & Barnea 1986).

The slug–churn transition

Churn flow was considered as a typical flow pattern in upward vertical and off-vertical gas–liquid flow. The above-mentioned model for slug–churn transition provides a quantitative explanation for the vanishing of churn flow in inclined pipes. Inclination of the pipe from the vertical causes the slug–churn boundary ([18] with $\alpha_s = 0.52$) and the annular–churn boundary (transition J) to move toward each other; and the churn flow shrinks and ultimately vanishes at relatively low liquid flow rates (figure 1). At very high liquid flow rates a region of intermittent flow with $\alpha_s \geqslant 0.52$ is observed in the whole range of pipe inclinations (figure 1). Although this region is usually not considered as the typical churn flow in experimental investigations, Brauner & Barnea (1986) suggested the possibility of designating this region also as churn flow.

The definition of churn flow as highly aerated slugs with repeated destruction of liquid continuity in the slug ($\alpha_s \geqslant 0.52$) is somewhat different from the usual association of churn flow with oscillatory motion of the liquid slug. There is, however, no contradiction between the two criteria since the oscillatory motion is caused by the high void fraction in the slug. However, the oscillatory motion is clearly observed only in vertical pipes and relatively low liquid flow rates, where gravity-dominated conditions exist. Yet the criteria of $\alpha_s = 0.52$, which cause destruction of the liquid slug, may be adopted as the criteria for churn flow in the whole range of pipe inclinations and flow rates.

The elongated bubble–slug transition

Slug flow which is free of entrained bubbles is considered as the elongated bubble flow pattern. The elongated bubble–slug transition is obtained by [18] with the limiting value of $\alpha_s = 0$. Equation [18] predicts the equilibrium gas void fraction within the main body of the liquid slug. However, at relatively high gas flow rates, especially in upward inclined and vertical flows, a local void concentration is developed behind the Taylor bubble due to the vigorous mixing region of the falling liquid film penetrating the liquid slug. Thus, the identification of elongated bubbles in upward flow may be ambiguous and not always consistent with the above definition. Because of this difficulty and because traditionally the distinction between elongated bubbles and slug was considered only in horizontal and slightly inclined flows, the predicted transition boundary is designated only for the horizontal case and is shown as curve N in figure 1 ($\beta = 0$).

SUBREGIONS IN THE STRATIFIED FLOW

Two subpatterns are usually defined in stratified flow: stratified smooth and stratified wavy. Waves may be formed on a smooth liquid interface due to the action of the gas flowing over the liquid (typical of horizontal tubes) or as a result of the action of gravity, even in the absence of gas flow (typical in downward inclined pipes).

Taitel & Dukler (1976a) suggested the following condition for wave generation as a result of the "wind" effect:

$$U_G \geqslant \left[\frac{4\,\nu_L(\rho_L - \rho_G)\rho\cos\beta}{s\,\rho_G\,U_L}\right]^{\frac{1}{2}}, \quad [19]$$

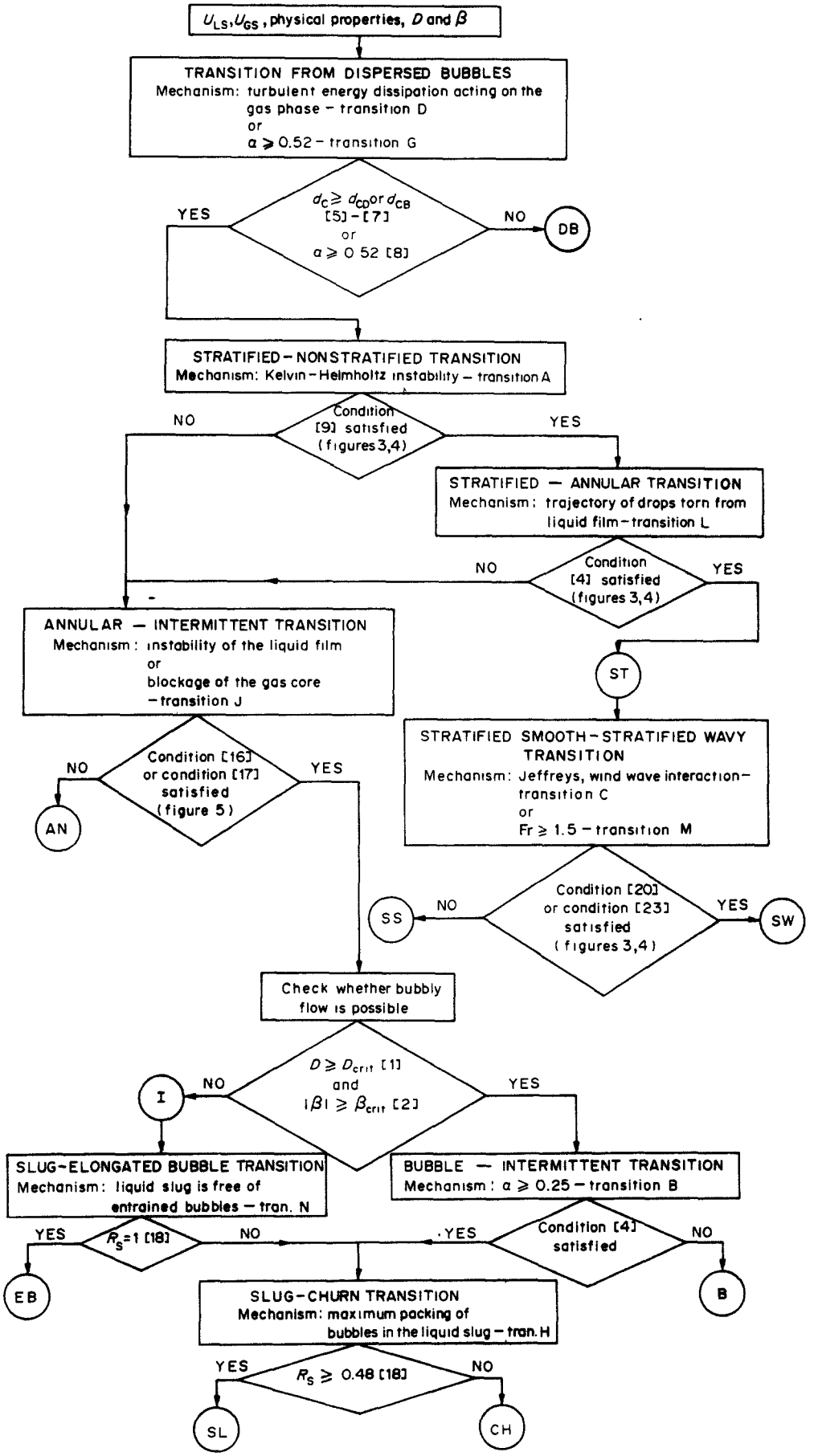

Figure 6. Logical pass for flow-pattern determination.

or in the dimensionless form

$$K \geqslant \left[\frac{2}{\tilde{U}_G \sqrt{\tilde{U}_L} \sqrt{s}}\right], \quad [20]$$

where ν_L is the liquid kinematic viscosity, s is a sheltering coefficient and K is the product of the modified Froude number and the square root of the superficial Reynolds number of the liquid:

$$K^2 = F^2 \, Re_{LS} = \left[\frac{\rho_G (U_{GS})^2}{(\rho_L - \rho_G) D g \cos\beta}\right]\left[\frac{D \, U_{LS}}{\nu_L}\right]. \quad [21]$$

All quantities in square brackets in [20] depend only on $\tilde{h}_L$. The transition between stratified smooth and stratified wavy resulting from the "wind" effect is mapped on a K vs $\tilde{h}_L$ coordinate system and is shown in figure 4 as curve C.

As has been mentioned, waves can be developed on liquid flowing in downward slopes, even in the absence of interfacial shear with gas flow. For turbulent flow in smooth pipes Barnea *et al.* (1982b) adopted the following criteria for wave inception:

$$Fr = \frac{U_L}{\sqrt{g h_L}} \geqslant 1.5 \quad [22]$$

or

$$W = \frac{U_{LS}}{\sqrt{gD}} \geqslant 1.5 \sqrt{\tilde{h}_L} \frac{\tilde{A}_L}{\tilde{A}}. \quad [23]$$

The r.h.s. of [23] depends only on $\tilde{h}_L$, thus the locus of W vs $\tilde{h}_L$ which satisfies [23] is the stratified smooth–stratified wavy transition boundary and is shown as curve M in figure 4.

Curves C and M are also plotted on U_{LS} vs U_{GS} coordinates for the air–water system at 25°C and 0.1 MPa (figure 1, $\beta = 0, -1$) and together give the composite stratified smooth–stratified wavy boundary. Note that at large gas flow rates transition M, where waves are formed due to the action of gravity, is terminated by transition C which represents the condition where waves are formed by interfacial shear. At inclination angles $> 5°$ both theory and experiments show that waves exist in the whole range of stratified flow.

THE UNIFIED MODEL

Transition mechanisms for each individual boundary and its applicability for the whole range of pipe inclinations have now been presented. These mechanisms have been used to arrive at operative equations or dimensionless maps which can be used to predict the transition boundaries between the flow patterns. These equations or maps incorporate the effect of flow rates, fluid properties, pipe size and the angle of inclination. A logical path for the systematic determination of the various flow patterns is presented by the flow chart shown in figure 6.

The flow patterns and the transition boundaries are shown in U_{GS}–U_{LS} space for the air–water system flowing in a 5 cm dia pipe (figure 1). The results of the model compare favorably with experimental data for the whole range of pipe inclinations. In the special case of tubes of small diameter where condition [1] is not satisfied, no bubbly flow can exist below curve D in vertical and off-vertical flows. This phenomena is also observed experimentally and is shown on the flow pattern map for a 2.5 cm dia tube (figure 2).

It should be noted that even when the mechanisms seem to be understood arriving at useful equations is not always a direct process and the final equations require estimations regarding some factors which enter into the mechanisms. For example, the transition mechanisms from separated flow (stratified or annular) require the inclusion of the friction factor f_i at the gas–liquid interface. The available relationships for f_i are largely empirical and limited to specific flow conditions. For the case of stratified flow f_i was assumed to equal the gas friction factor coefficient, f_G, for the whole range of pipe inclinations (Taitel & Dukler 1976a), although the choice of $f_i = f_G$ applies mainly to separated smooth flow. For the case of annular flow, Wallis' (1969) correlation for f_i was used for the whole range of pipe inclinations and flow conditions (Barnea 1986), although it applies to symmetric annular flow with high gas flow rates. Presently there are no confirmed data that

correlate f_i with the wavy structure of the interface which can be expressed by the relative phase velocity, the film thickness and the pipe inclination. Therefore use of the available correlations for f_i was made for the whole range of inclinations and flow conditions with some sacrifice of accuracy.

REFERENCES

BARNEA, D. 1986 Transition from annular and from dispersed bubble flow—unified models for the whole range of pipe inclinations. *Int. J. Multiphase Flow* **12,** 733–744.

BARNEA, D. & BRAUNER, N. 1985 Holdup of the liquid slug in two phase intermittent flow. *Int. J. Multiphase Flow* **11,** 43–49.

BARNEA, D., SHOHAM, O. & TAITEL, Y. 1982a Flow pattern transition for vertical downward two phase flow. *Chem. Engng Sci.* **37,** 741–746.

BARNEA, D., SHOHAM, O. & TAITEL, Y. 1982b Flow pattern transition for downward inclined two phase flow; horizontal to vertical. *Chem. Engng Sci.* **37,** 735–740.

BARNEA, D., SHOHAM, O. & TAITEL, Y. 1985 Gas–liquid flow in inclined tubes: flow pattern transitions for upward flow. *Chem. Engng Sci.* **40,** 131–136.

BRAUNER, N. & BARNEA, D. 1986 Slug/churn transition in upward vertical flow. *Chem. Engng Sci.* **41,** 159–163.

HARMATHY, T. Z. 1960 Velocity of large drops and bubbles in media of infinite or restricted extent. *AIChE Jl* **6,** 281–288.

HUSAIN, A. & WEISMAN, J. 1978 Applicability of the homogeneous flow model to two phase pressure drop in straight pipe and across area changes. *AIChE Symp. Ser., No. 174* **74,** 205–214.

KADAMBI, V. 1982 Stability of annular flow in horizontal tubes. *Int. J. Multiphase Flow* **8,** 311–328.

LIN, P. Y. & HANRATTY, T. J. 1986 Prediction of the initiation of slugs with linear stability theory. *Int. J. Multiphase Flow* **12,** 79–98.

MCQUILLAN, K. W. & WHALLEY, P. B. 1985 Flow patterns in vertical two phase flow. *Int. J. Multiphase Flow* **11,** 161–175.

MISHIMA, Y. & ISHII, M. 1984 Flow regime transition criteria for two phase flow in vertical tubes. *Int. J. Heat Mass Transfer* **27**(5), 723–736.

SHOHAM, O. 1982 Flow pattern transitions and characterization in gas–liquid two phase flow in inclined pipes. PhD. Dissertation, Tel-Aviv Univ., Ramat-Aviv, Israel.

STREETER, V. L. 1961 *Handbook of Fluid Dynamics*. McGraw-Hill, New York.

TAITEL, Y. 1977 Flow pattern transitions in rough pipes. *Int. J. Multiphase Flow* **3,** 597–601.

TAITEL, Y. & DUKLER, A. E. 1976a A model for prediction flow regime transition in horizontal and near horizontal gas–liquid flow. *AIChE Jl* **22,** 47–55.

TAITEL, Y. & DUKLER, A. E. 1976b A theoretical approach to the Lockhart–Martinelli Correlation for stratified flow. *Int. J. Multiphase Flow* **2,** 591–595.

TAITEL, Y., BARNEA, D. & DUKLER, A. E. 1980 Modeling flow pattern transitions for steady upward gas–liquid flow in vertical tubes. *AIChE Jl* **26,** 345–354.

WALLIS, G. B. 1969 *One-dimensional Two-phase Flow*. McGraw-Hill, New York.